Eur. Phys. J. B **51**, 307–313 (2006)
DOI: 10.1140/epjb/e2006-00227-5

THE EUROPEAN PHYSICAL JOURNAL B

The structural and electronic properties of compound Sn_mO_n clusters studied by the Density Functional Theory

A.M. Mazzone[a] and V. Morandi

CNR, IMM, Sezione di Bologna, via Gobetti 101, 40129 Bologna, Italy

Received 20 January 2006 / Received in final form 31 March 2006
Published online 13 June 2006 –

Abstract. The purpose of this study is the assessment of the properties of compound Sn_mO_n clusters (m = 1, 2, 3, 4 and n = 1,..,10) and is justified by the theoretical and practical importance of the crystalline stannic oxides and of the related silicon-oxygen systems. The optimized structure is obtained from the minimization of the total energy evaluated using the Density Functional Theory. The quantities analyzed are the cluster structure, its binding energy, the spatial distribution of the electronic charge and the density of states. This analysis indicates that the cluster structure consists on two approximately separate sublattices. In agreement with this central feature, the size dependence of the parameters of the electronic charge is well described by superposing the corresponding values for the elemental clusters.

PACS. 61.46.Bc Clusters – 78.20.Bh Theory, models, and numerical simulation – 71.15.Mb Density functional theory, local density approximation, gradient and other corrections

1 Introduction

The structural and electronic properties of clusters represent an important field in condensed matter physics and attention has been given to clusters formed by almost all the available elements and also compound structures have been considered. The trust of studies of this last group is the development of materials with novel structural, electronic and magnetic properties with respect to either the bulk case or the clusters of the pure elements. Furthermore these researches are also in line with studies of a fundamental character directed at the prediction and systematization of compounds (see [1,2] and references therein).

Earlier works in the physical literature centered on clusters formed by simple metals containing one heteroatom. For instance, clusters involving alkaline metal hosts with an aluminum and magnesium impurity atom and aluminum clusters with a nitrogen heteroatom were considered in [3] and [4], respectively. The aim of these studies was the understanding of the perturbation produced by the heteroatom in the light of the predictions of the simple jellium model. At the present state of the art, the focus of the researches on compound clusters is on the elements of the group IV. In fact, while Si and Ge clusters are important for semiconductor devices, Sn and Pb are useful for soldering and doping provides an useful tool to manipulate these properties at the nanoscale. Calculations at semi-empirical level have been developed for cyclic clusters with a skeletal part formed by Si, Ge, Sn and Pb to state their aromatic properties in comparison with the ones of hydrocarbons [5]. Hypersilicon clusters (i.e. clusters of composition Si_mO with m = 2, 3) have been studied to investigate their analogy with hypermetallic molecules (i.e. molecules of composition Y_mX where Y = Li, Na, K, Mg, Al and X is an electronegative atom) and to clarify how oxygen atoms and molecules react with various silicon surfaces [6]. Calculations with a different level of accuracy have been developed for fullerenes, and analogous silicon cages, containing an endohedral impurity and for silloxenix clusters (i.e clusters of composition Si, H, O)(see [7–9] and references therein). More recently, a detailed characterization of ten atom clusters of Si, Ge, Sn and Pb doped with Ni or Pt has been presented and the aim of this study was to clarify the capability of encapsulation of these clusters known to be magic [10].

The focus of the present study is on clusters of a mixed tin-oxygen composition. In fact, the elements of the group IV can, in addition to displaying the +4 oxidation state expected for their group, displaying an oxidation state of two lower. For Sn this is demonstrated by the occurrence of the two oxides SnO and SnO_2, which are known to crystallize under ambient conditions in a layered and rutile structure, respectively. However accurate experimental observations shows also the formation of Sn_mO_n compounds with m, n varying in the range 1–3 and 2–12, respectively [11]. It is therefore of both practical and conceptual importance to state which compositions are stable in the clustered state. The following calculations illustrate structural and electronic properties of stable compound clusters and dwell on the features of heterogeneous bonding in comparison with bonding in the elemental clusters.

[a] e-mail: mazzone@bo.imm.cnr.it

2 The computational methods

As mentioned above, compound structures considered in the literature consist on a small aggregate of host atoms containing only one additive. The issues addressed by these calculations are if the heteroatom is coordinated outside or inside the host cluster and which structural changes of the cluster structure and binding strength are produced by these configurations. At variance with this strategy, this study attempts to approach the more general problem of the miscibility of two AB elements by considering clusters formed by a similar number of A and B atoms (in the following $m = metal$, $n = nonmetal$, N and $x = m/n$ indicate the number of tin and oxygen atoms, the cluster size and the stoichiometric ratio between the number of tin and oxygen atoms, respectively). According to this choice, the number of tin and oxygen atoms vary in the range to $m = 1, 2, 3, 4$ and $n = 1, 2, 3m$. The values $n = 1, 2m$ are consistent with the stoichiometry of the bulk oxides whereas $n = 3m$ is somewhat speculative and has to be seen as the asymptotic limit of the overconcentration of one of the two elements.

Clusters studies clearly indicate that the evaluation of a global minimum of the potential energy surface is a delicate task, due to the large number of parameters to be optimized. For compounds the further degrees of freedom arising from composition leads to an exponential growth of the possible structures, with an obvious increase of the computational burden. Generally, these problems are dealt with starting the search for a minimum from families of structures chosen on the basis of a plausible physical behavior and for compounds the obvious choice is the shape of the stable elemental clusters. This approach has also been adopted in this work. The structures used to start the minimization are the stable tin clusters and the compound structure is generated by inserting oxygen atoms, dimers and trimers in a bridging position between tin atoms. Alternatively, the oxygen subclusters were positioned externally to the tin skeleton or, for the larger sizes, the shape of a small fragment of crystalline SnO_2 was also used.

The evaluation of clusters total energy is based on the Density Functional Theory (DFT) using SIESTA [15]. In these recent years DFT with the Local Density Approximation (LDA) for the correlation-exchange potential has become a central approach in solid state physics and has been successfully applied to a wide variety of solids, nanostructures and molecular systems. In spite of the deep understanding offered by these calculations, they have also shown systematic errors, most notably an overestimation of the binding energy. A known source of this error is the LDA potential and significant improvements are achieved by the Generalized Gradient Approximation (GGA), which has also the advantages of a simple formulation and easy to use. However controversial results on the accuracy of GGA and LDA are reported for tin-based materials. In fact the study of high-pressure properties of tin, using SIESTA, shows that correct results on the structure and elastic properties are obtained from LDA while GGA accurately reproduces the experimental binding energies [16]. On the other side the DFT-LDA study of the cohesion of tin monoxide and dioxide shows relevant changes of the elastic parameters in dependence of the formulation of the pseudopotential [17]. This correction, however, needs the guidance of experimental data and its application to clusters is unsafe. Furthermore Hartree-Fock studies of tin clusters suggest that a correct evaluation of the binding energy can be obtained using the standard pseudopotential formulation provided that scalar relativistic effects are included [20]. A further known source of errors in both DFT and Hartree-Fock (HF) calculations is the Basis Set Superposition Error (BSSE) which arises from the limited size of the basis set by necessity adopted in the calculations. No result directly comparable with ours is reported for BSSE. The only available suggestion is offered by the HF study of CO adsorption onto SnO_2 in [18], which indicates that the BSSE error on the molecule adsorption energy is in the range 0.1 eV.

To assess the accuracy of our calculations an extensive testing was carried out on the parameters needed by DFT and a comparison between DFT and Hartree Fock calculations was also made. Unless otherwise specified the SIESTA inputs are: a mesh cutoff of 80.0 Ry, the Troullier-Martins nonlocal pseudopotentials in the Kleinman-Bylander form with or without the relativistic corrections, the Ceperley-Alder correlation functional with the Perdew-Zunger parameterization or the Perdew-Burke-Ernzerhof functional (indicated below as LDA or GGA, respectively). The electronic configuration of Sn and O is $5s^2 5p^2 4d^{10}$ and $2s^2 2p^4$ with a cut-off radius of the core pseudopotential equal to 1.90 and 1.55 a.u., respectively. A spin-polarized distribution of charge was adopted in both LDA and GGA. The basis sets used in SIESTA are formed by Slater-type Pseudo-Atomic Orbitals (PAO) constructed from the eigenstates of the atomic potential. A comparison among PAO with a different accuracy, i.e. single or double-ζ with or without polarization (indicated as Sζ, Dζ, SζP, DζP, respectively), was regularly made as an empirical estimate of BSSE.

The method implemented in the package GAMESS [19] has been used for the Hartree-Fock calculations (this choice is motivated by the high-level calculations on tin clusters reported in [20]). In GAMESS core states are represented by the effective Hay-Wadt potential and the Coulomb and exchange potentials are evaluated directly from the valence charge density. The basis set are Slater-type orbitals with atomic parameters. An important option offered by GAMESS is that the search for a minimum can be be started from an optimized geometry obtained from a semi-empirical Hamiltonian. The MNDO Hamiltonian contained in MOPAC has been used to this purpose [21,22]. Generally, first order-geometries were calculated with MNDO and successively refined with SIESTA. GAMESS was applied to the structures obtained from either MNDO or SIESTA.

The quantities reported below illustrate the cluster structure and its electronic configuration and are of common use in the cluster literature. The structural

parameters are the average, maximum and minimum interatomic distance, d_{av}, d_{max} and d_{min}, respectively. These distances, on their whole, are indicative of the cluster size and symmetry and of its bonding mode. A further parameter mentioned below is the aspect ratio. The aspect ratio quantifies the cluster asymmetry and is evaluated from the ratio between the inertial moments with respect to two in-plane equatorial axes. The parameters of the electronic configuration are the Mulliken charges and dipole moments, the binding energy and the density of states, i.e. DQ, D, E_b and DOS (by DQ we indicate specific components of the Mulliken charge whose meaning is defined when they are used). E_b is the total energy of the system evaluated with respect to a similar system of free atoms. Its meaning is analogous to the cohesive energy of solids as it shows the quality of bonding and the cluster stability. Furthermore the calculations are performed at zero temperature so that E_b represents also the total energy in the ensembles of common use in statistical physics [23]. DQ and D are indicative of the spatial distribution of the charge whereas the DOS shows its orbital composition.

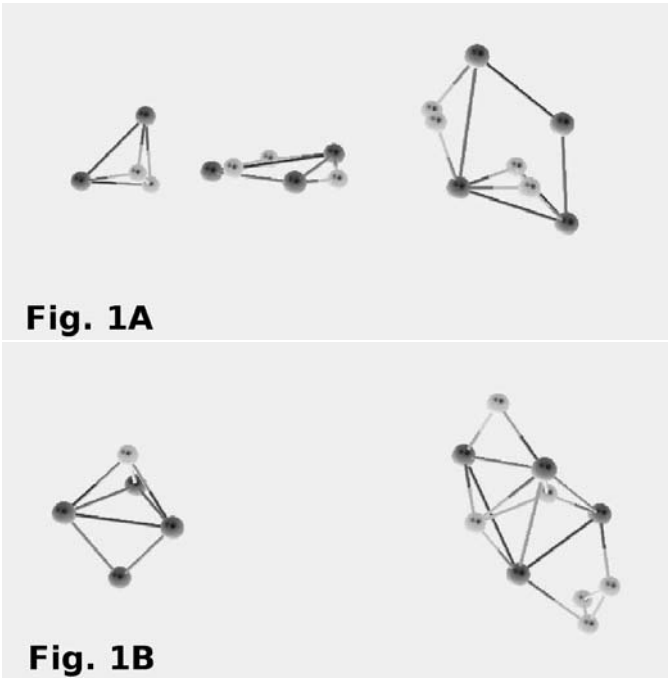

Fig. 1. The structure of Sn_nO_m clusters: the clusters reported in (A) are: Sn_2O_2, Sn_3O_3, and Sn_4O_4. The ones in (B) are: Sn_4O, $Sn4O_6$. The tin and oxygen atoms are marked by the paler and darker spheres, respectively.

3 The compound clusters: structure and electronic configuration

To set the stage briefly, it is recalled that, under the spur of the many studies on silicon clusters, also the properties of tin clusters have been carefully investigated for a systematization of the group IV elements. Their properties up to the size 50 have been analyzed by the use of *ab initio* HF, DFT and semiempirical calculations and in experiments. A detailed description of the electronic structure, including the higher moments of spin-orbit coupling, of tin clusters with $N \leq 5$ can be found in [20,25,26]. DFT calculations are reported in [27,28] and a comparison between silicon and tin is reported in [24] and related works. Other references are cited in [12]. As for silicon, the structure of the tin clusters is sustained by hybrid sp^3 bonds and the shape of the clusters with $N \leq 7$ is equal in the two elements. In both Si and Sn, in fact, the shape for $N = 3$ and $N = 4$ is a triangle and a rhombus, respectively, and larger clusters are formed by tetrahedral units sharing an edge. The tin bondlength is slightly larger than the one of silicon (the values are around 2.7 and 2.3 Å, respectively) and the absolute value of the binding energy is smaller. For tin E_b decreases irregularly with N and attains the cohesive energy of the solid (i.e. 3.14 eV) at $N \sim 12$. As for oxygen, the O_2 molecule, owing to its unusual triplet state, has been studied frequently in its gas, liquid or solid phase in theory and experiments (earlier and more recent bibliography can be found in [29,30] and [31], respectively). It is underlined that the large number of electrons of tin and the complex spin configuration of oxygen makes the calculations of Sn-O systems naturally prone to errors. In fact, the experimental value of the binding energy for Sn_2 is -1.2 eV/atom and its GGA and LDA evaluations are -1.21 and -2.9 eV/atom, respectively. Similarly, E_b of O_2, whose experimental value is -2.62 eV/atom, can be overestimated by DFT up to -3.73 eV/atom [29]. However the DFT evaluation of the structural properties is correct and for both the tin clusters and the O_2 molecule the error on the bondlengths is in the range few percents with respect to the experimental data.

Considering these features in the context of this study, the small shape of the oxygen clusters (the O_2 bondlength is 1.18 Å) suggests that the compound clusters retain the skeleton of the tin clusters and the oxygen atoms are embedded in this skeleton. Furthermore the high binding strength of O_2 and the molecular structure of O_4 [31] indicate a splitting of the oxygen subcluster into distant parts. Therefore the electronic structure of the compound cluster derives from the separate contributions of the oxygen and tin subclusters, a part from corrections due to charge exchange and hybridization. Literature results are in agreement with this description. In fact, in the chemical literature it is reported that the heavier atoms have a low tendency to form hybrid orbitals even in compounds (the so-called 'inert ns^2-electron pair effect [5]). In the affine case of the hypersilicon clusters of composition Si_mO [6] the silicon skeleton remains intact and the oxygen coordinates outside this skeleton. The calculations reported below confirm, on their whole, these features though relevant differences are also observed.

The quantities reported in the following figures are: the cluster structure (Fig. 1), the internuclear distances and dipole moment (Fig. 2), the binding energy (Figs. 2–4) and the DOS (Fig. 5). Generally, it was found that clusters of all sizes and composition are in a bonded state with

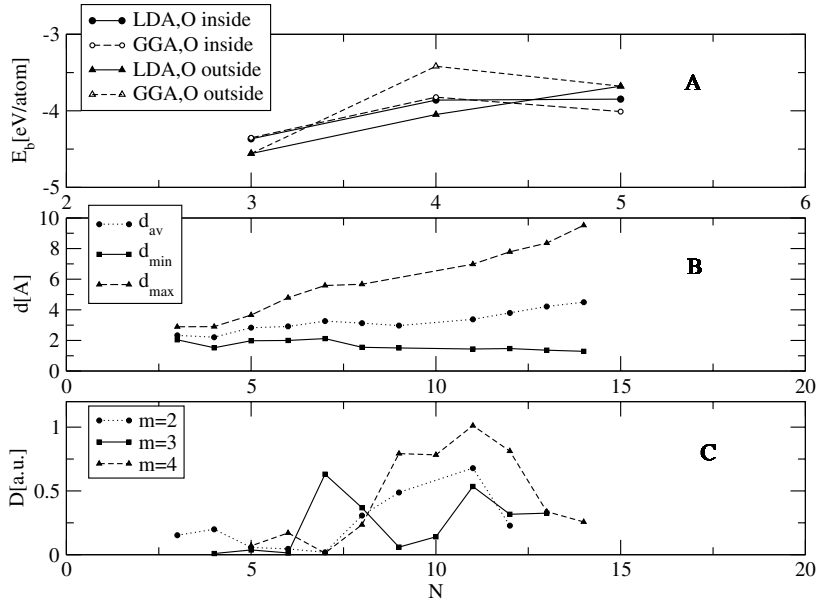

Fig. 2. Panel (A): the binding energy of the clusters Sn_mO with $m = 2$, 3, 4 for the conditions shown. Panel (B): the internuclear distances d_{av}, d_{min} and d_{max} in the three groups of structures with tin atoms equal to $m = 2$, 3, 4 . DFT calculations. Panel (C): the dipole moment D in the three groups above. DFT calculations.

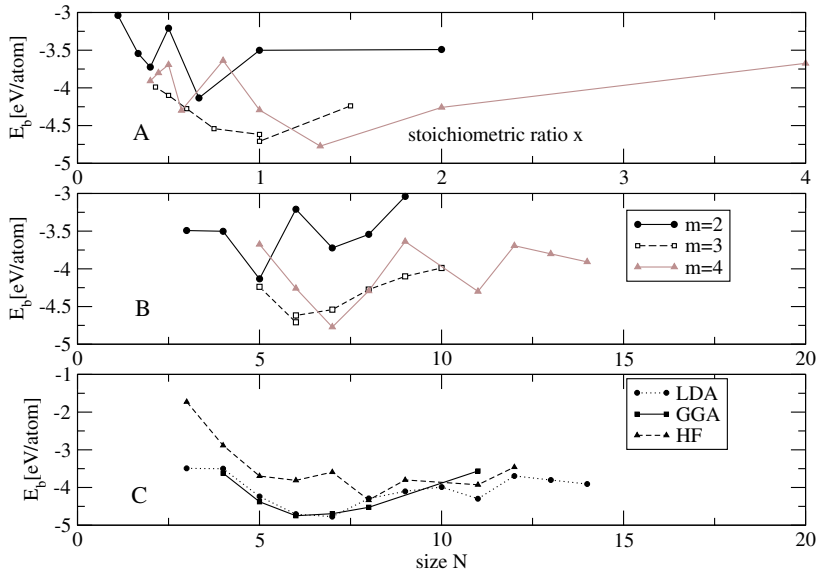

Fig. 3. Panel (A): the binding energy as a function of the stoichiometric ratio x in the three groups of structures with a number of tin atoms $m = 2$, 3, 4. DFT calculations. Panel (B): the binding energy as a function of the size N. Same conditions as in panel A. Panel (C): the minimum binding energy in the three groups above. DFT and HF calculations.

an E_b value remarkably smaller than the one of the elemental clusters Sn_3, Sn_4 (whose values are -2.60, -2.84 eV/atom in the LDA estimate). However at each size an abundant series of nearly isomeric shapes, with an E_b difference in the range a few tenth of eV, was also found. No clear dependence between the relaxed structure and the one adopted to start the minimization was found. Though a detailed description of all these shapes is impossible, an useful systematization has been found separating the clusters where oxygen coordinates prevalently outside or inside the tin subclusters. The stability of these two cluster types derives from the balance between bonding and antibonding interactions and has a complex dependence on the cluster size and composition.

These properties are illustrated in Figures 1 and 2. The lattice views in Figure 1 refer to clusters of size N up to 10. In Figure 1A the stoichiometric ratio x is equal to one as the clusters composition is Sn_mO_m with $m = 2$, 3, 4. On the contrary, the clusters reported in Figure 1B refer to a large and a small value of x, i.e. $x = 4$ and 0.67, and the cluster composition is Sn_4O and Sn_4O_6. The analysis of the bondlengths of these clusters shows that in all cases the tin-tin and oxygen-oxygen distances increase of some percents with respect to their values in the pure clusters. Accordingly, the interaction between the tin and oxygen subcluster has a partially repulsive character which however does not greatly modify the originally binding strength of the elemental subclusters. From Figure 1A it is also seen that the increase of N favors structures with oxygen coordinated inside, rather than outside, the tin subcluster. This feature is also proved by the evaluation of the binding energy reported in Figure 2A. These calculations refer to the clusters Sn_mO with $m = 1$, 2, 3, where the oxygen atom is coordinated outside and inside

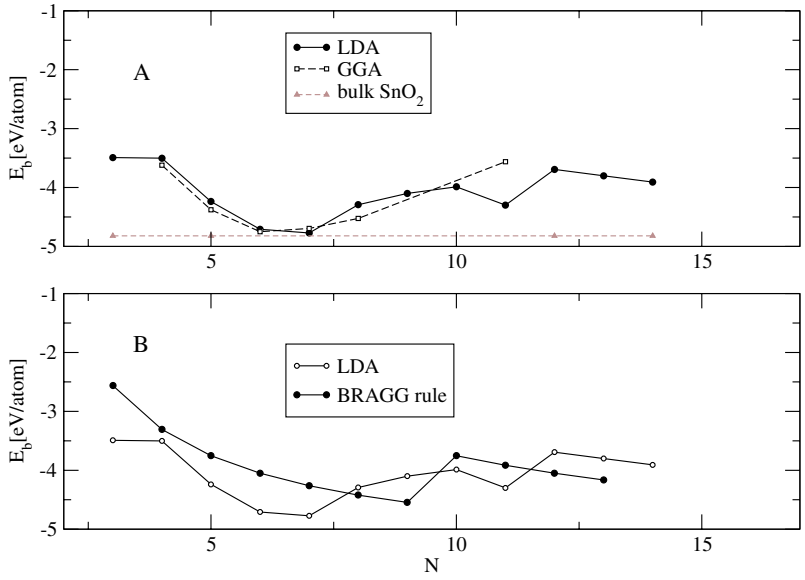

Fig. 4. Panel (A): the minimum binding energy in the three groups $m = 2$, 3, 4. DFT calculations. The bulk limit is also shown. Panel (B): the binding energy evaluated using the Bragg rule.

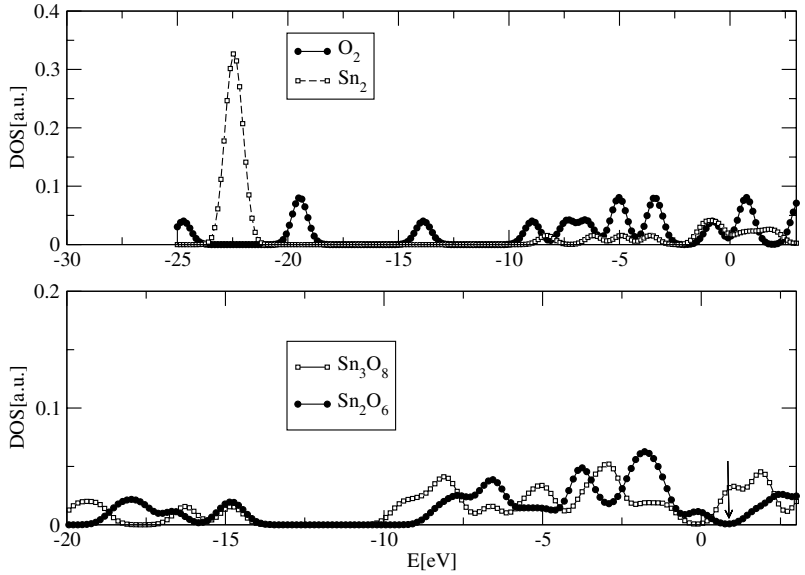

Fig. 5. The DOS of pure and compound clusters. The top panel shows the DOS of Sn_2 and O_2 and the bottom one the DOS of Sn_2 O_2 and Sn_2 O_6.

the cluster structure. This last configuration appears energetically favored at the larger N and these calculations indicate that a fairly large size is required to encapsulate one oxygen atom. The energy gain is however modest, in the range 0.5 eV/atom. The effect of the oxygen additives on the tin skeleton is illustrated by the comparison of Figures 1A and 1B. In Figure 1A for $m = 4$ the four member ring of the tin atoms has the rombohedral shape of the elemental Sn_4 cluster whereas it acquires a pyramidal shape in Figure 1B. This structure represents a stable configuration on the potential energy surface of Sn_4 but is higher in energy than the rombohedral one due the antibonding contributions arising from the formation of dihedral angles. Its stabilization in the compound clusters arises from Sn-O interactions and the comparison of Sn_4O and Sn_4O_6 shows that the addition of only one oxygen atom is sufficient to produce the pyramidal shape. However, while Sn_4 is the elemental cluster with lowest binding energy for the sizes considered in this study, the E_b values of the compounds containing Sn_4, i.e. Sn_4O and Sn_4O_4 are -3.674, -4.29 eV/atom, respectively. These values are representative. They indicate that an optimal stoichiometric ratio is needed to preserve a progression of the binding energy with m equal to the one of the elemental clusters. As shown below, this conclusion is also supported by a more detailed evaluation of the binding energy.

A quantitative formulation of the structural properties of clusters and of their size dependence is offered by the internuclear distances (Fig. 2B). As mentioned above, at the smaller sizes, owing to the scarce hybridization of the bondlenghts, the average and minimum distances d_{av} and d_{min} retain the values of the pure tin and oxygen clusters.

The increase of the cluster size leads to the increase of d_{av} and d_{max} and this last one is much sharper than the former. In our structures the increase of N is prevalently due to the oxygen content and therefore the increase of d_{max} arises from the oxygen atoms. However even in those cases the cluster has a compact structure as the aspect ratio is generally around one. Furthermore the values of the dipole moment D (Fig. 2C) are of one order of magnitude larger than the ones in the silicon clusters of the same size [34] which indicates an uneven charge distribution in the compound clusters. For these clusters the smaller D values are at the smaller or at the larger N. In these asymptotes the cluster composition is dominated by the tin or the oxygen atoms, respectively. Therefore the high values of D at intermediate N are due to the charge imbalance between the two subclusters, rather than to their separate contributions. This indicates a mixed covalent-ionic type of bonding in this range of sizes.

The plots in Figures 3, 4 illustrate the dependence of the binding energy on the cluster size and composition. In Figures 3A and 3B the values of E_b in the groups with a number of tin atoms $m = 2$, 3 and 4 are plotted as a function of x and N, respectively. The calculations in Figure 3C show the minimum values attained in these groups and a comparison between different theoretical models is also made. The oscillatory behaviour of E_b (Figs. 3A and 3B) is accounted for by the critical nature of the stoichiometric ratio, as explained above. However the existence of 'magic' elements is also evident. The group with $m = 4$ has the lower binding energies and there is an optimum stoichiometric ratio x around one. Whereas the optimum $m = 4$ is attributable to the stability of Sn_4, the optimum x is determined by the inherent stability of the two subclusters and is supported by analytical theories on compounds. In fact, a simple but insightful relationship to evaluate the stability of compound structures is offered by the Bragg rule which has been extensively applied to metallic elements in their bulk phase [33]. In this formulation the total energy E of a binary compound formed by the element A and B can be expressed as $E = x_A V_{AA} + x_B V_{BB}$ where x_A and x_B are the concentration of the elements A and B and V_{AA} and V_{BB} the corresponding on-site energies. This expression can be adapted to the binding energies in the form $E_b = mE_{Sn} + nE_O$ where E_{Sn} and E_O represent the strength of the tin and oxygen bonds. The plot of this energy, obtained using for E_{Sn} and E_O the E_b values of the tin and oxygen dimer, is presented in Figure 4B where a comparison with DFT calculations and with the bulk limit is also made (Fig. 4A). A good agreement is observed and the main divergence of the analytical formulation is that the minimum is only slight displaced from $N = 7$, 8 towards $N = 8$, 9. This result is obviously attributable to the scarce sensitivity of the analytical formulation to the details of the bonding in the clusters.

The analysis of the Mulliken charges in the elemental tin clusters showed that the overlapping charge DQ has values in the range 0.50 and 0.30 for nearest and second nearest neighbours interactions, respectively. Similar dQ values are observed also for the compound clusters. These hybrids charges suggest a complex structure of DOS, which is also a known property of the rutile lattice (reported, for instance, in [9]). In this case, in fact, owing to the mixed ionic and covalent character of bonding, the DOS plot shows a separation of the O $2p$ and Sn $5p$ states across the Fermi energy and the admixture of O $2p$ and Sn $5s$ ones above it. In Figure 5 a comparison is made between the DOS plot of the pure clusters and of the compound ones (the pure clusters are O_2 and Sn_2 and the compound clusters are Sn_2O_4 and Sn_2O_6). In the first case, the more evident feature of DOS is a structured shape with many peaks produced by the slight broadening of the atomic levels. In the compound clusters the overlapping of these peaks leads to the formation of bands located across the Fermi energy (the zero in the energy scale). The width of these bands is scarcely responsive to the cluster size and composition but a shift towards the higher energy is generally produced by the increase of the oxygen content. A further common feature is a small gap at the Fermi energy (marked with an arrow in Fig. 5) which is in line with a semiconductor behaviour.

To conclude this section a few remarks on the accuracy of the calculations are also in order. From the computational point of view our calculations are in qualitative and quantitative agreement with literature results. In fact, as quoted at the beginning of this section, the literature data indicate the overbinding of the LDA, which equally appears in solids and clusters. Our calculations follow the known trend and the overbinding is reduced on passing from LDA to GGA whereas HF leads to a small underbinding (Fig. 3C). It is however underlined that the LDA evaluation approaches the cohesive energy of crystalline SnO_2 at N around 7 (Fig. 4A). This feature is realistic and is also exhibited by the tin clusters. It therefore appears that LDA leads to more correct results in the case of compounds than for the pure clusters. Minor effects arise from pseudopotentials and basis sets. In fact, as reported in [16], the inclusion of nonlinear core corrections in the tin pseudopotential does not qualitatively alter the cluster structure and has only some influence at a qualitative level on E_b. The fluctuations of E_b arising from the use of DζP, instead of Dζ or Sζ basis sets, are around 10%. As the former set is more complete than the latter ones, this result suggests that BSSE has a limited role in our calculations. At variance with the binding energy, the evaluation of the structure is stable and the fluctuations of the bondlengths arising from the parameters of the DFT formulation fall in the range few percents.

4 Conclusions

In this study the properties of stable Sn_mO_n clusters have been presented and analyzed. The calculations offer some insight, to be developed in future studies, on the plausible trends of structures with a complex bonding configuration. The results indicate that the formation of a compound cluster has minor effects on the structural properties as the tin and oxygen subclusters retain the characteristic lengths of the clusters of the pure elements. Also the size

dependence of the binding energy can be described by a simplistic superposition of the binding strength of the two components and this also applies to the DOS structure.

This research project, code RBAUO1M974, is partially supported by MIUR.

References

1. W. Andreoni, G. Galli, M. Tosi, Phys. Rev. Lett. **55**, 1734 (1985)
2. A. Zunger, Phys. Rev. B **22**, 5839 (1980)
3. B.K. Rao, P. Jena, Phys. Rev. B **37**, 2867 (1988)
4. S.K. Nayak, S.N. Khanna, P. Jena, Phys. Rev. B **57**, 3787 (1988)
5. S. Nagase, Pure and Appl. Chem. **65**, 4, 7, 675 (1993)
6. A.I. Boldyrev, J. Simons, J. Phys. Chem. **97**, 5875 (1993)
7. S. Nagase, K. Kobayashi, Chem. Phys. Lett. **187**, 3, 291 (1991)
8. M.R. Pederson, W.E. Pickett, S.C. Erwin, Phys. Rev. B **48**, 17400 (1993)
9. A.M. Mazzone, Europhys. Lett. **35**, 13 (1996)
10. V. Kumar, A.B. Singh, Y. Kawazoe, Nanoletters **4**, 677 (2004)
11. M. Launay, F. Boucher, P. Moreau, Phys. Rev. B **69**, 35101 (2004)
12. A.M. Mazzone, Comp. Mat. Science **21**, 211 (2001); and also Phil. Mag. Lett. **82**, 99 (2002); ibid. **84**, 275 (2004)
13. E.L. Peltzer Blanca', A. Svane, N.E. Christensen, C.O. Rodriguez, O.M. Capannini, M.S. Moreno, Phys. Rev. B **48**, 15712 (1993)
14. W. Dazhi, W. Shulin, C. Jun, Z. Suyan, L. Fangqing, Phys. Rev. B **49**, 14282 (1994)
15. J.M. Soler, E. Artacho, J.D. Gale, A. Garcia, J. Junquera, P. Ordejon, D. Sanchez-Portal, J. Phys.: Condens. Matter **14**, 2745 (2002)
16. A. Aguado, Phys. Rev. B **67**, 212204 (1981)
17. M. Meyer, G. Onida, M. Palummo, L. Reining, Phys. Rev. B **64**, 45119 (2001)
18. M. Melle-Franco, G. Pacchioni, Surf. Sci. **461**, 54 (2000)
19. M.W. Schmidt, K.K. Baldridge, J.A. Boatz, S.T. Elbert, M.S. Gordon, J.H. Jensen, S. Koseki, N. Matsunaga, K.A. Nguyen, S.J. Su, T.L. Windus, M. Dupuis, J.A. Montgomery, J. Comp. Chem. **14**, 1347 (1993)
20. D. Dai, K. Balasubramanian, J. Phys. Chem. **100**, 19321 (1996)
21. MOPAC Quantum Chemistry Program Exchange: Program Number 571. Other information can be found at the web site `www.indiana.edu`
22. J.P. Stewart, J. Comp. Chem. **10**, 209 (1989)
23. Y.C. Kim, M.E. Fisher, E. Luijten, Phys. Rev. Lett. **91**, 651, 2003
24. K.A. Jackson, M. Hiroi, I. Chauduri, T. Fraunenheim, A.A. Shvartsburg, Phys. Rev. Lett. **93**, 13401 (2004)
25. K. Balasubramanian, K.S. Pitzer, J. Chem. Phys. **78**, 321 (1985)
26. G. Pacchioni, Mol. Phys. **55**, 211 (1985)
27. Zhong-Yi Lu, Cai-Zhuang Wang, Kai-Ming Ho, Phys. Rev. B **61**, 2329 (2000)
28. C. Majumder, V. Kumar, H. Mizuseki, Y. Kawazoe, Phys. Rev. B **64**, 233405 (2001)
29. E. Wimmer, H. Krakauer, M. Weinert, A.J. Freeman, Phys. Rev. B **2**, 864 (1981)
30. G.S. Painter, F.W. Averill, Phys. Rev. B **26**, 1781 (1982)
31. V. Aquilanti, D. Ascenzi, M. Bartolomei, D. Cappelletti, E. Cavalli, M. de Castro Vitores, F. Pirani, Phys. Rev. Lett. **82**, 69 (1999)
32. J.P. Perdew, A. Savin, K. Burke, Phys. Rev. B **51**, 4531 (1995)
33. D.C. Chrzan, L.M. Falicov, Phys. Rev. B **37**, 3894 (1988)
34. J.R. Chelikowsky, D.J. Chadi, M. Biggeli, Phys. Rev. B **64**, R2051 (2000)